Catalytic Activity of Palladium Nanoparticles Encapsulated in Spherical Polyelectrolyte Brushes and Core−Shell Microgels

Yu Mei, Yan Lu, Frank Polzer, and Matthias Ballauff*

Physikalische Chemie I, University of Bayreuth, 95440 Bayreuth, Germany

Markus Drechsler

Makromolekulare Chemie II, University of Bayreuth, 95440 Bayreuth, Germany

Received October 26, 2006. Revised Manuscript Received December 22, 2006

We present a quantitative comparison of the catalytic activity of palladium nanoparticles immobilized in different colloidal carrier systems, namely, in (i) spherical polyelectrolyte brushes (SPB) and (ii) core−shell microgels. The first system given by the SPB carrier particles consist of a solid core of polystyrene onto which long chains of poly((2-methylpropenoyloxyethyl) trimethylammonium chloride) (PMPTAC) are grafted. These positively charged polyelectrolyte chains form a dense layer on the surface of the core particles which binds the divalent $PdCl_4^{2-}$ ions. Reduction leads to metallic Pd particles. System 2 is given by core−shell microgels which consists of a solid core of polystyrene and a shell of cross-linked poly(*N*-isopropylacrylamide) (PNIPA). The metal ions were strongly localized within the network because of complexation of the $PdCl_4^{2-}$ ions and the nitrogen atoms of PNIPA. Reduction of these ions leads to nearly monodisperse nanoparticles of metallic palladium that are only formed within the polymer layer. The average diameter *d* of the particles is approximately 2.4 nm (system 1; SPB) and 3.8 nm (system 2; microgel). Both types of composite particles exhibit an excellent colloidal stability. The catalytic activities of the Pd nanoparticles in both carrier systems were investigated by monitoring photometrically the reduction of *p*-nitrophenol by an excess of $NaBH_4$. We find that the catalytic activity of the palladium nanoparticles is strongly influenced by the carrier system: The measured rate constants of Pd nanoparticles immobilized in spherical polyelectrolyte brushes (system 1) is much higher than the one measured for Pd particles in the network of the microgels (system 2). The dependence of the rate constants obtained for both carrier systems demonstrates that these differences must solely be traced back to the different diffusional barriers in both carrier systems; there is no indication for any specific interaction of the polymer chains with the metallic nanoparticles. A comparison with data from literature demonstrates that both types of core−shell particles are excellent carrier systems that may be used to tune the catalytic activity of the metallic nanoparticles.

1. Introduction

Recently, much attention has been focused on metal nanoparticles such as gold, platinum, and palladium because their properties may markedly differ from the ones of the respective bulk metals.[1] These metal nanoparticles exhibit size-induced quantum-size effects (i.e., electron confinement and surface effect)[1,2] and can be exploited for a number of advanced functional applications as sensors[3] and in electronics and catalysis.[4,5] The formation of metal nanoparticles is commonly carried out by reduction of metal ions in the presence of a stabilizer like polymers,[6] dendrimers,[7,8] microgels,[9] surfactants,[10] and colloids,[11,12] which prevent the nanoparticles from aggregation and serve as carriers. In general, the catalytic properties of metal nanoparticles are a function of their size, crystal lattice parameters, and properties of carrier systems.[13,14] In many respects, composite systems from organic carrier molecules and metallic nanoparticles present a novel class of materials that must have the following properties: On the one hand, stabilizing agents should not alter or block the surface of the nanoparticles. On the other hand, carrier systems should be sufficiently stable to ensure the recycling of the catalyst after reaction.

Recently, we showed that well-defined gold and platinum nanoparticles can be generated in spherical polyelectrolyte particles.[15,16] No coagulation takes place during the genera-

* Corresponding author. E-mail: matthias.ballauff@uni-bayreuth.de.

(1) Burda, C.; Chen, X.; Narayanan, R.; El-Sayed, M. A. *Chem. Rev.* **2005**, *105*, 1025.
(2) Kamat, P. V. J. *Phys. Chem. B* **2002**, *106*, 7729.
(3) Frederix, F.; Friedt, J.; Choi, K.; Laureyn, W.; Campitelli, A.; Mondelaers, D.; Maes, G.; Borghs, G. *Anal. Chem.* **2003**, *75*, 6894.
(4) Praharaj, S.; Nath, S.; Ghosh, S.; Kundu, S.; Pal, T. *Langmuir* **2004**, *20*, 9889.
(5) Campbell, C. T.; Parker, S. C.; Starr, DE. *Science* **2002**, *298*, 811.
(6) Li, Y.; Boone, E.; El-Sayed, M. A. *Langmuir* **2002**, *18*, 4921.
(7) Esumi, K.; Isono, R.; Yoshimura, T. *Langmuir* **2004**, *20*, 237.
(8) Zhao, M.; Crooks, R. M. *Angew. Chem., Int. Ed.* **1999**, *38*, 364.
(9) Zhang, J.; Xu, S.; Kumacheva, E. J. *Am. Chem. Soc.* **2004**, *126*, 7908.
(10) Bonnemann, W.; Brijoux, A.; Schulze, T.; Siepen, K. *Top. Catal.* **1997**, *4*, 217.
(11) Liang, Z.; Susha, A.; Caruso, F. *Chem. Mater.* **2003**, *15*, 3176.
(12) Kidambi, S.; Bruening, M. L. *Chem. Mater.* **2005**, *17*, 301.
(13) Semagina, N.; Joannet, E.; Parra, S.; Sulman, E.; Renken, A.; Kiwi-Minsker, K. *Appl. Catal., A* **2005**, *280*, 141.
(14) Kralik, M.; Biffis, A. *J. Mol. Catal. A* **2001**, *177*, 113.
(15) Sharma, G.; Ballauff, M. *Macromol. Rapid Commun.* **2004**, *25*, 547.
(16) Mei, Y.; Sharma, G.; Lu, Y.; Ballauff, M.; Drechsler, M.; Irrgang, T.; Kempe, R. *Langmuir* **2005**, *21*, 12229.

10.1021/cm062554s CCC: $37.00
Published on Web 02/10/2007

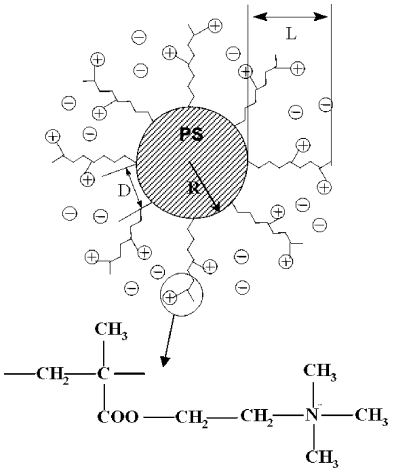

Figure 1. Scheme of the spherical polyelectrolyte brush (SPB) used in this study. The particles consist of a PS core and PMPTAC polyelectrolyte chains densely attached to these cores. The average distance D between two brush chains is much smaller (ca. 2−6 nm) than the contour L_c of the chains. Hence, the limit of a polyelectrolyte brush is reached in these systems.

tion of the nanoparticles on these particles. Figure 1 shows the structure of the spherical polyelectrolyte brush particle in a schematic manner: Long cationic polyelectrolyte chains are chemically grafted to colloidal polystyrene particles. The polyelectrolyte chains affixed to the surface of the carrier particles is very dense; that is, the contour length L_c of the chains is much higher than their average distance on the surface of the carrier particle (see Table 1). In this way a polyelectrolyte "brush" results, which denotes a system of strongly interacting polymer chains grafted densely to a planar or curved surface.[17] The counterions derived from the synthesis can be replaced by suitable ions of noble metals such as $AuCl_4^-$ or $PtCl_6^{2-}$. The confinement of the counterions can now be used to remove a possible surplus of metal ions outside the brush particles by ultrafiltration. Subsequent reduction of the metal ions to the metal nanoparticles can be achieved by suitable reagents like $NaBH_4$.[14,15,17] Figure 2 shows the generation of metallic nanoparticles on spherical polyelectrolyte brushes in a schematic manner.

More recently, a second way of immobilizing metallic nanoparticles was presented: We generated silver nanoparticles in thermosensitive microgel particles, which consist of polystyrene (PS), whereas the network consists of poly(*N*-isopropylacrylamide) cross-linked by *N*,*N*′-methylenebisacrylamide (BIS).[18,19] Figure 2 displays a scheme of these composite systems and their synthesis. The catalytic activity of the silver nanoparticles encapsulated in these particles has a distinct non-Arrhenius-like dependence on temperature: On one side, the raising temperature will accelerate the activities of silver particles; on the other side, the PNIPA network will shrink at elevated temperature, leading a marked barrier for the diffusion of the reactants. Thus, the rate constant showed an S-curve as the function of temperature.[18,19]

Evidently, a quantitative comparison of the catalytic activity of nanoparticles of a given metal in both systems will reveal the influence of the colloidal carriers. In particular, such a comparison must immediately lead to information on whether the catalytic activity of a given metal nanoparticle is directly influenced by the carrier or whether the carrier may just provide a barrier for the diffusion of the educts and the products. Quantitative information of the catalytic activity of nanoparticles in different carriers under well-controlled conditions hence provides the first step for the rational design of "smart" composite particles and materials that act as carriers as well as switches for the activity of the nanoparticles.

In this paper we carry out such an analysis for palladium nanoparticles: We compare the catalytic activity of palladium nanoparticles embedded in different carrier systems as shown schematically in Figure 2. Palladium nanoparticles of similar size are generated in spherical polyelectrolyte brushes (system 1) as well as in a thermosensitive microgel system (system 2) and compared with regard to their catalytic activity. As a model reaction, we chose the reduction of *p*-nitrophenol by excess sodium borohydride that can be easily monitored by UV/ vis spectroscopy.[7,16,18−21] In this way the influence of the carrier system on the catalytic activity of the nanoparticles will become evident. Moreover, since this reaction has been used in other studies as well, the results given here can be directly compared to recent investigations that have employed different strategies of immobilization of the metal particles.

2. Experimental Section

2.1. Materials. *N*-Isopropylacrylamide (NIPA, Aldrich), *N*,*N*′-methylenebisacrylamide (BIS, Fluka), sodium dodecyl sulfate (SDS, Fluka), and potassium peroxodisulfate (KPS, Fluka) were used as received. Styrene (BASF) was destabilized by an Al_2O_3 column and stored in a refrigerator. Sodium tetrachloropalladate (Na_2PdCl_4, Aldrich) and reducing agent sodium borohydride ($NaBH_4$, Aldrich) were used as received. *p*-Nitrophenol (reagent grade) was obtained from Aldrich and used as received. Water was purified using reverse osmosis (MilliRO, Millipore) and ion exchange (MilliQ, Millipore) and served as deionized water.

2.2. Synthesis of the Thermosensitive Microgel. The thermosensitive microgel PS-NIPA was synthesized and characterized as described recently.[18,19,22] PS core latex was prepared by conventional emulsion polymerization using styrene (253.2 g) and NIPA (13.75 g) as monomers, SDS (2.34 g dissolved in 925 g of water) as surfactant, and KPS (0.50 g dissolved in 20 g of of water) as initiator. The reaction was run at 80 °C for 8 h. Purification was done by ultrafiltration with 10 times the volume of water. The core−shell system was prepared by seeded emulsion polymerization. PS core latex (347.67 g) was diluted with 500 g of water together with 40.07 g of NIPA and 1.37 g of BIS. After that, the mixture was heated to 80 °C, the reaction was started with the addition of 0.40 g of KPS (dissolved in 15 g of water), and continued for 4.5 h. The latex was purified by serum replacement against deionized

(17) Advincula, R. C.; Brittain, W. J.; Caster, K. C.; Rühe, J. *Polymer Brushes*; Wiley-VCH: Weinheim, 2004.
(18) Lu, Y.; Mei, Y.; Ballauff, M.; Drechsler, M. *Angew. Chem.* **2006**, *45*, 813.
(19) Lu, Y.; Mei, Y.; Drechsler, M.; Ballauff, M. *J. Phys. Chem. B* **2006**, *110*, 3930.
(20) Pradhan, N.; Pal, A.; Pal, T. *Colloids Surf. A* **2002**, *196*, 247.
(21) Ghosh, S. K.; Mandal, M.; Kundu, S.; Nath, S.; Pal, T. *Appl. Catal. A* **2004**, *268*, 61.
(22) Dingenouts, N.; Seelenmeyer, S.; Deike, I.; Rosenfeldt, S.; Ballauff, M.; Lindner, P.; Narayanan, T. *Phys. Chem. Chem. Phys.* **2001**, *3*, 1169.

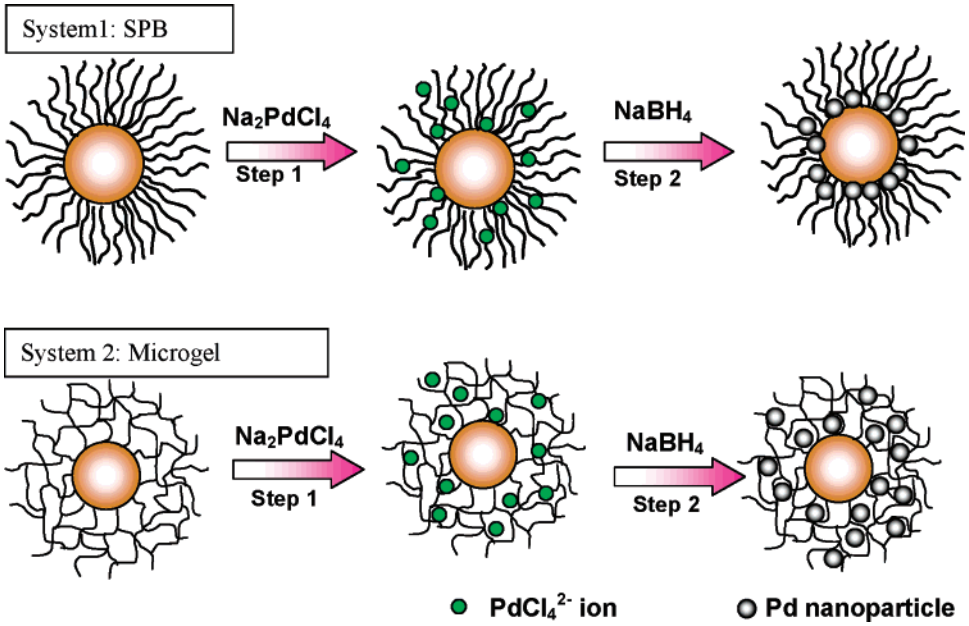

Figure 2. Schematic representation of formation of palladium nanoparticles in spherical polyelectrolyte brushes (SPB) or microgels. The upper part shows the SPB that has a shell of poly((2-methylpropenoyloxyethyl) trimethylammonium chloride). The metal ions, namely, $PdCl_4^{2-}$, are confined within the brush layer. Reduction of the metal ions by $NaBH_4$ leads to nanosized palladium particles bound on the PS surface. The lower part shows the microgel particles which has a network-like shell consisting of PNIPA cross-linked by BIS. Palladium nanoparticles were generated and confined within the PNIPA network-like shell.

Table 1. Characterization of the Spherical Polyelectrolyte Brush Particles[a]

label	charge	R [nm]	L_c [nm]	M_w [g/mol]	σ [nm^{-2}]	D [nm]	L_c/R
SPB-30	positive	46	182	150800	0.019	8.2	3.96

[a] R: core radius of polystyrene; M_w: molecular weight of grafted chains; L_c: contour length of grafted chains determined from M_w; σ: graft density on surface of polystyrene core; D: the average distance between two neighboring graft points.

Table 2. Preparation of Palladium Nanoparticles

sample	carrier particles [g]	particle size[c] [nm]	water [g]	$NaBH_4$ [g]	Na_2PdCl_4 [mol/L]
Microgel-1-Pd9[a]	4.0	130	196.0	0.038	5.0×10^{-4}
SPB-30-Pd9[b]	3.0	191	97.0	0.038	5.0×10^{-4}

[a] The solid content of Microgel-1 is 4.60%. [b] The solid content of SPB-30 latex is 15.22%. [c] The particle size was measured by dynamic light scattering at 20 °C.

water (membrane: cellulose nitrate with 100 nm pore size supplied by Schleicher & Schuell).

2.3. Synthesis of Palladium Nanoparticles Using SPB as Carrier Particles (System 1). After the synthesis and purification of the SPB particles, suspensions thereof were washed with Na_2PdCl_4 solution (5.0×10^{-4} mol/L) of at least 10 times volume, which ensures that all counterions in the brush were replaced with $PdCl_4^{2-}$. Then the $PdCl_4^{2-}$ ions in brush particles were reduced by $NaBH_4$ under an atmosphere of nitrogen. Here a tenfold excess of $NaBH_4$ (see Table 2) was added slowly to the suspension at room temperature with vigorous stirring. Typically, the addition of $NaBH_4$ was done within 30 min. The onset of reaction could be seen from a slight change of color of the suspension which became grayish. After the last addition the latexes were stirred for another 1 h and then cleaned by serum replacement against deionized water (membrane: cellulose nitrate with 100 nm pore size supplied by Schleicher & Schuell). This process removed the salt introduced by the synthesis as well as a fraction of free palladium particles formed outside of polyelectrolyte brush.

2.4. Synthesis of Palladium Nanoparticles Using Microgel as Carrier Particles (System 2). Na_2PdCl_4 solution (5.0×10^{-4} mol/L) was added to the purified microgel after synthesis. The mixture was homogenized using a magnetic stirrer for at least 2 h until the color of mixture did not change anymore, which indicates that all $PdCl_4^{2-}$ ions formed complexation with the nitrogen atoms of the PNIPA shell of the microgel. Under an atmosphere of nitrogen a tenfold excess of $NaBH_4$ (see Table 2) was added slowly to the suspension at room temperature with vigorous stirring. Typically, the addition of $NaBH_4$ was done within 30 min. The color of the mixture soon changed from orange to grayish. After the last addition the latexes were stirred for another 1 h and then cleaned by serum replacement against deionized water (membrane: cellulose nitrate with 100 nm pore size supplied by Schleicher & Schuell) to remove residual salts in the system and free palladium particles outside the microgel.

2.5. Catalytic Reduction of *p*-Nitrophenol. As a model reaction, we chose the reduction of *p*-nitrophenol by $NaBH_4$ to *p*-aminophenol. In a typical run, a given amount of palladium nanoparticles was added to a solution of *p*-nitrophenol (0.1 mmol/L). After mixing of these solutions, a given amount of sodium borohydride (10 mmol/L) was added to start the reduction. The kinetic process of the reduction was monitored by measuring the extinction of solution at 400 nm as the function of time. To study the effect of oxygen dissolved in water on the kinetics, nitrogen was used to purge water for 30 min. $NaBH_4$ was added directly into the solution to start the reaction.

2.6. Characterization of Pd-Composite Particles. The Pd-composite particles were characterized by dynamic light scattering, UV/vis spectroscopy, Cryo-TEM, and FESEM after purification. Dynamic light scattering measurements were performed with ALV 4000 (Peters) under 90°. The UV spectra of *p*-nitrophenol were measured by a Lambda 25 spectrometer (Perkin-Elmer) at different temperatures. Cryo-TEM specimens were prepared by vitrification of thin liquid films supported on a TEM copper grid (600 mesh, Science Services, Munich, Germany) in liquid ethane at its freezing

Table 3. Catalytic Activity of the Palladium Nanoparticles: Comparison with the Literature[a]

sample	T [°C]	k_{app} [s^{-1}]	k_1[b] [$s^{-1}\,m^{-2}\,L$]	c [mmol/L]	d [nm]	S[b] [m^2/L]	ref
Microgel-1-Pd9	15	1.50×10^{-3}	1.01×10^{-1}	2.15×10^{-3}	3.8 ± 0.6	1.49×10^{-2}	this work
SPB-30-Pt3	15	3.47×10^{-3}	5.62×10^{-1}	6.60×10^{-4}	2.1 ± 0.4	8.58×10^{-3}	15
SPB-30-Pd9	15	4.41×10^{-3}	1.10	3.66×10^{-4}	2.4 ± 0.5	4.00×10^{-3}	this work
PAMAM Dendrimer G 4.0	15	1.79×10^{-3}	3.07×10^{-3}	2.00×10^{-2}	1.8 ± 0.42	5.83×10^{-1}	7
PPI Dendrimer G 3.0	15	4.07×10^{-1}	7.76×10^{-1}	2.00×10^{-2}	2.0 ± 0.41	5.25×10^{-1}	7

[a] k_{app}: apparent rate constant; k_1: rate constant normalized to the surface of the particles in the system (see eq 1); d: diameter of the palladium particles; S: surface area of palladium nanoparticles normalized to the unit volume of the system; c: total amount of palladium particles in the system. [b] Calculated from the data given in the respective papers.

point. The specimen was inserted into a cryotransfer holder (CT3500, Gatan, Munich, Germany) and transferred to a Zeiss EM922 EFTEM (Zeiss NTS GmbH, Oberkochen, Germany). Examinations were carried out at temperatures around 90 K. The TEM was operated at an acceleration voltage of 200 kV. All images were recorded digitally by a bottom-mounted CCD camera system (UltraScan 1000, Gatan, Munich, Germany) and processed with a digital imaging processing system (Digital Micrograph 3.9 for GMS 1.4, Gatan, Munich, Germany). A Carl-Zeiss TGZ3 particle counter was used to estimate particle size of palladium nanoparticles from TEM images. Field-emission scanning electron microscopy (FESEM) was performed using a LEO Gemini microscope equipped with a field emission cathode. The amount of pure palladium particles was determined by TGA; at first, latex was dehydrated in a dry oven; then about 15 mg of solid composites were heated to 1000 °C under 30.0 mL/min nitrogen by a METTLER TOLEDO STARe System. The heating-up speed was adjusted to 10°C/ min. The bulk density of palladium was used ($\rho = 12.16 \times 10^3$ kg/m^3; ref 23) in the calculation of surface area of palladium nanoparticles.

3. Results and Discussion

3.1. Morphology of Palladium Nanoparticles Embedded in SPB and Microgel. Figure 2 summarizes the method of generating nanoparticles on the surface of spherical polyelectrolyte brush and thermosensitive microgel in a schematic manner.[16] The generation of the nanoparticles takes place within the polymer layer; virtually no particles are formed outside. For the spherical polyelectrolyte brush (system 1), the counterions derived from the synthesis can be replaced by $PdCl_4^{2-}$. The confinement of the counterions can be used to remove a possible surplus of metal ions outside the brush particles by ultrafiltration.[16] This strong localization of the $PdCl_4^{2-}$ ions within the PNIPA polymer network shell of system 2 is caused by a complexation of the $PdCl_4^{2-}$ ions by the nitrogen atoms of the PNIPA.[24]

The reduction to metallic nanoparticles in both systems was done at room temperature through addition of $NaBH_4$ and could be seen from a slight darkening of the suspensions. All systems remained stable during the reaction and the subsequent cleaning by ultrafiltration. In general, the composite particles exhibited the same colloidal stability as the unmodified SPB or microgel particles. The good stability was also found in the subsequent studies of the catalytic activity. It is the main prerequisite for the use of these composite particles in catalysis.

While the ordinary TEM micrographs display only particles in which the dry layer of polymer shell has been collapsed, cryo-TEM shows the particles in situ. Figure 3 displays the TEM micrographs obtained for both carrier systems. In the case of the brush particles (system 1; Figures 3c and 3d), practically all palladium nanoparticles are located near the surface of the core particles. This finding points to the fact that there must be a marked dispersion attraction between the nanoparticles and the cores. Obviously, the palladium nanoparticles encounter no difficulties in reaching the polystyrene core surface since the polyelectrolyte brush has an open structure. In contrast, in the case of PNIPA particles shown in Figures 3a and 3b the palladium particles cannot reach the surfaces of the polystyrene cores because they are immobilized in the dense PNIPA network. Moreover, the analysis of the cryo-TEM micrographs showed that the palladium nanoparticles embedded in spherical polyelectrolyte brush have a size of 2.4 ± 0.5 nm. For the thermosensitive microgels we obtained the slightly higher value of 3.8 ± 0.6 nm. Hence, the size range is comparable in both cases.

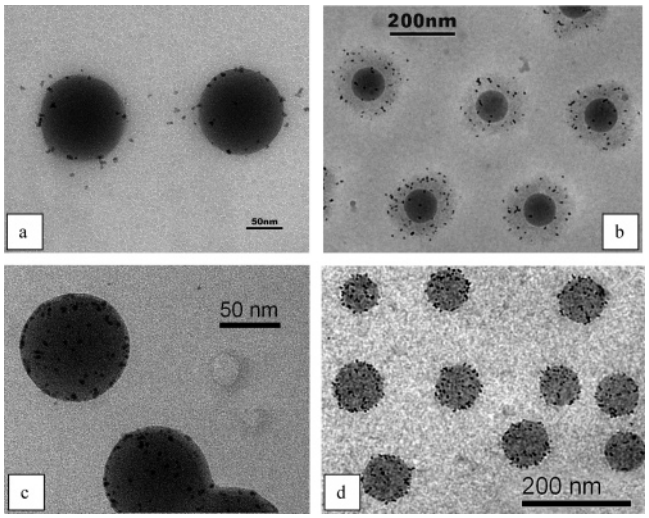

Figure 3. Electron microscopy images of palladium nanoparticles encapsulated in different templates. (a, b) TEM and Cryo-TEM images of palladium nanoparticles encapsulated in PNIPA latex particles. (c, d) TEM and Cryo-TEM images of palladium nanoparticles encapsulated in PMPTAC latex particles.

3.2. Effect of Concentration of Palladium Nanoparticles on the Catalytic Activity of the Reduction of *p*-Nitrophenol. Having discussed the synthesis and the morphology of the palladium composite particles, we now turn to the catalytic properties of these particles. As a model reaction, we used the reduction of *p*-nitrophenol by an excess of $NaBH_4$. In this way the results can directly be compared to the data supplied in the literature.[7,16,18] The rates of reduction were assumed to be independent of the concentration of

(23) Weast, R. C. *Handbook of Chemistry and Physics*; CRC Press: Cleveland, 1975; p B-27.
(24) Beck, W. *Pure Appl. Chem.* **1988**, *60*, 1357.

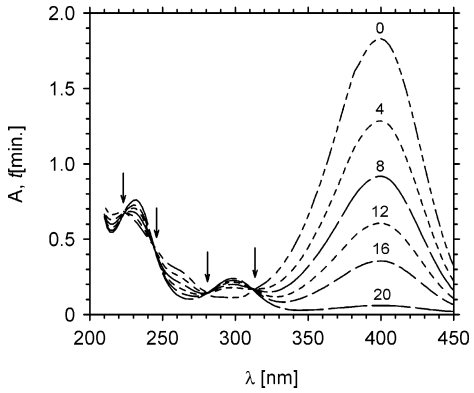

Figure 4. Spectra of *p*-nitrophenol in the presence of the composite particles SPB-30-Pd9 as catalyst. The absorbance A_t measured at different time t (in minutes) indicated in the graph is plotted against the wavelength λ. Four isosbestic points were found at 224, 244, 281, and 313 nm. This indicates that *p*-aminophenol is the unique product of the reduction. The concentrations of the reactants were as follows: [*p*-nitrophenol] = 0.1 mmol/L, [$NaBH_4$] = 10 mmol/L, [Pd composites] = 0.24 mg/L, T = 20 °C.

sodium borohydride since this reagent was used in large excess compared to *p*-nitrophenol.[21] Therefore, the kinetic data were fitted by a first-order rate law. Moreover, the apparent rate constant k_{app} was assumed to be proportional to the surface S of the metal nanoparticles present in the system,

$$-\frac{dc_t}{dt} = k_{app}c_t = k_1 S c_t \quad (1)$$

where c_t is the concentration of *p*-nitrophenol at time t and k_1 is the rate constant normalized to S, the surface area of metal nanoparticles normalized to the unit volume of the system. This allows us to compare systems with different content of nanoparticles. Figure 4 demonstrates that the kinetics of the reduction can easily be monitored by UV/vis spectroscopy. Four isosbestic points are visible, showing that the reduction proceeds without byproducts.

With use of platinum and silver composite particles as catalysts in reduction of *p*-nitrophenol, the reaction does not start immediately but only after some delay that is due to the oxygen dissolved in water.[16,18,19] This delay time t_0 was also observed for both systems studied here, namely, palladium nanoparticles encapsulated in spherical polyelectrolyte brushes and thermosensitive microgels. Oxygen dissolved in water reacts with $NaBH_4$ presumably much faster while *p*-nitrophenol does not react. Thus, extinction of the system does not change with time in the first period. Only when all O_2 has been consumed will *p*-nitrophenol be reduced. In all experiments reported herein, oxygen was therefore removed from water by purging the solutions by a flow of nitrogen for 30 min. After this, the reaction was started by addition of $NaBH_4$ directly to the reaction mixture in the UV/vis spectrometer. The delay time t_0 disappears after exclusion of oxygen dissolved in water. This can be seen directly from Figures 5a and 5b, showing the plots according to eq 1 for both systems.

3.3. Comparison of Catalytic Activity of Palladium Nanoparticles Encapsulated in Different Carriers. The catalytic activities normalized to the surface area of different

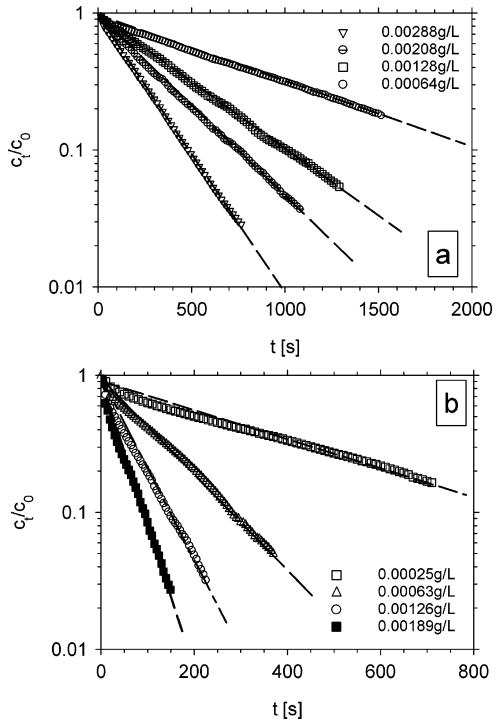

Figure 5. Influence of palladium-composites particles concentration on the reduction of *p*-nitrophenol. The concentrations of the reactants were as follows: [*p*-nitrophenol] = 0.1 mmol/L, [$NaBH_4$] = 10 mmol/L, T = 20 °C. (a) Kinetics of reduction of *p*-nitrophenol under catalysis of the Microgel-1-Pd9 system. (b) Kinetics of reduction of *p*-nitrophenol under catalysis of the SPB-30-Pd9 system.

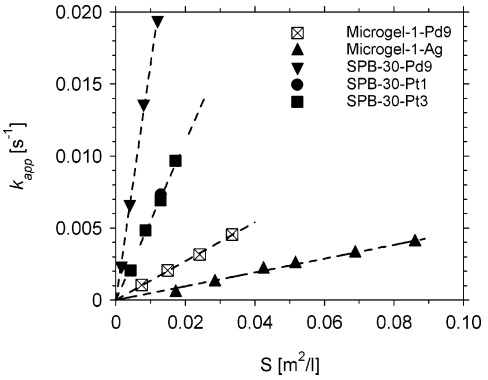

Figure 6. Rate constant k_{app} as the function of surface area S of metal nanoparticles normalized to the unit volume of the system (see eq 1).

composite particles obtained from Figure 5 according to eq 1 are summarized in Figure 6. For this purpose the rate constants k_{app} obtained from Figures 5a and 5b and from the literature[18] were normalized to the surface area in unit volume of the system using the bulk density of palladium ($\rho = 12.16 \times 10^3$ kg/m^3; ref 23). Therefore, Figure 6 displays these results in a plot of k_{app} versus the surface S of the metal particles. First of all, the palladium particles immobilized in spherical polyelectrolyte brushes (SPB-30-Pd9 in Figure 6) exhibit a higher catalytic activity than platinum nanoparticles encapsulated in the same system (SPB-30-Pt1 and Pt3 in Figure 6), both taken from ref 16. A similar comparison could be made for metallic nanoparticles encapsulated in microgels. Here we found that the catalytic activity of palladium nanoparticles is higher than the one of silver nanoparticles (Microgel-1-Pd9 and Microgel-1-Ag; see Figure 6). This

shows that the catalytic activities depend on the kind of metal regardless of the type of carrier system. In all cases, the order of reactivity is palladium > platinum > silver (see also refs 16 and 18).

On the other hand, Figure 6 demonstrates that palladium nanoparticles embedded in polyelectrolyte and thermosensitive microgel systems (system SPB-30-Pd9 and Microgel-1-Pd9) have totally different catalytic activities. This can be explained by the diffusion speed of reactant molecules to metal nanoparticles encapsulated in both carrier systems. In the case of polyelectrolyte system 1 that has an open structure, reactant molecules can diffuse in latex particles and reach metal nanoparticles more quickly while in the case of network-like PNIPA shell, that is, system 2, reactant molecules need a longer time to reach the catalytic active center. That means that catalytic activities of embedded metal nanoparticles are strongly affected by the carrier systems. We shall address the reasons for this marked difference when discussing the dependence on temperature. All kinetic data obtained herein are summarized in Table 3.

We now compare the activity of our palladium nanoparticles immobilized in different carriers to data given in the literature. As mentioned above, kinetic data are available on the reduction of *p*-nitrophenol with $NaBH_4$ under comparable conditions. To arrive at a meaningful comparison, all data have been reduced to the total surface of the metal nanoparticles in the system according to eq 1. The respective data are gathered in Table 3.

Esumi et al. stabilized silver, platinum, and palladium nanoparticles in PPI or PAMAM dendrimers with various generations.[7] Using the third generation of PPI dendrimers (see Table 5 of ref 7) as carrier system, Esumi et al. obtained palladium nanoparticles of 2.0 ± 0.41 nm that were used as catalyst in reduction of *p*-nitrophenol by excess $NaBH_4$. With 2.0×10^{-2} mmol/L palladium nanoparticles (5.25×10^{-1} m^2/L, recalculated from ref 7) the highest value of the rate constant $k_{app} = 4.07 \times 10^{-1}$ s^{-1} was obtained at 15 °C. This value decreases, however, if more dendrimer is used for the stabilization of the particles (see Table 5 of ref 7). Hence, the catalytic activity of dendrimer−metal composite nanoparticles depends on concentration and generation of the dendrimer as well as the surface functional groups of the dendrimer. The rate constants for the PPI dendrimer−platinum and −palladium nanocomposites are significantly greater than the ones obtained for the PAMAM dendrimer−platinum and −palladium nanocomposites.[7] The magnitude of the rate constants for both PPI and PAMAM dendrimers is palladium > platinum > silver.[7]

Zhao and Crooks[8] synthesized palladium nanoparticles in the presence of G4-OH dendrimer. These particles are narrowly distributed (1.3 ± 0.3) nm and were used as catalyst in hydrogenation of alkenes in aqueous solutions. They found that the hydrogenation rate constant can be controlled by using dendrimers of different generations. It can be explained by the hindrance of substrate penetration by sterically crowded terminal groups of higher generation dendrimers.[8]

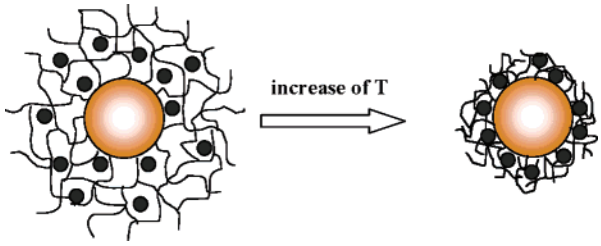

Figure 7. Schematic representation of microgel−Pd composite particles consisting of thermosensitive microgel particles in which palladium nanoparticles are embedded. The composite particles are suspended in water which swells the thermosensitive network attached to the surface of the core particles. In this state the reagents can diffuse freely to the nanoparticles that act as catalyst. At higher temperatures (T > 30 °C) the PNIPA network shrinks and the catalytic activity of the nanoparticles is diminished in this state.

The results summarized in Table 3 can be compared since all nanoparticles are of similar size. It needs to be noted that reduction to k_l (fourth column of Table 3) reduced all data to the same surface of the nanoparticles. The comparison given in this table demonstrates that the Pd nanoparticles immobilized in the brush particles exhibit a much higher activity that the ones immobilized within the microgel particles. Moreover, it is obvious that Pd nanoparticles are slightly more active than the platinum nanoparticles studied in ref 15. The reason for this significant difference between different metals is not yet clear and further studies are needed. In general, the activity of the nanoparticles immobilized by dendrimers is smaller, in particular if PAMAM dendrimers have been used for the stabilization. Again this is a problem in need of further clarification. It might point to a stronger interaction of the dendrimers with the surface of the nanoparticles that could reduce their activity.

3.4. Effect of Temperature on the Catalytic Activity of the Reduction of *p*-Nitrophenol. The thermosensitive microgel particles are suspended in water that swells the PNIPA at room temperature. The PNIPA network, however, undergoes a volume transition around 32 °C in which most of the water is expelled. Figure 7 shows this transition in a schematic fashion. Earlier experiments have demonstrated that this transition is perfectly reversible.[25,26] Hence, the process of shrinking and re-swelling can be repeated without degradation or coagulation of the particles.

Measurements of composite particles by dynamic light scattering at different temperatures indicate that the original thermosensitive properties of PNIPA network are not hindered by the incorporation of palladium particles into the network. Figure 8 displays the hydrodynamic radii of the carrier particles (quadrangles) and the composite particles (circles). Both sets of data agree showing that the thermosensitive shell undergoes the volume transition at 32 °C. This is in agreement with previous findings.[26,27] Obviously, the palladium nanoparticles do not disturb the volume transition within the network. This suggests that the interaction of the network with the Pd particles is weak. We conclude that there is no pronounced additional cross-linking that takes place

(25) Dingenouts, N.; Norhausen, C.; Ballauff, M. *Macromolecules* **1998**, *31*, 8912.
(26) Ballauff, M. *Macromol. Chem. Phys.* **2003**, *204*, 220.
(27) Deike, I.; Ballauff, M.; Willenbacher, N.; Weiss, A. *J. Rheol.* **2001**, *45*, 709.

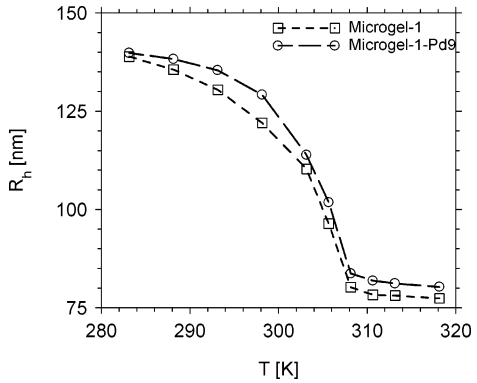

Figure 8. Hydrodynamic radii of Microgel-1-Pd9 composite particles (system 2) at different temperatures measured by dynamic light scattering at 90°. Quadrangles give the hydrodynamic radii for the carrier particles (Microgel-1) and hollow circles for composite particles (Microgel-1-Pd9).

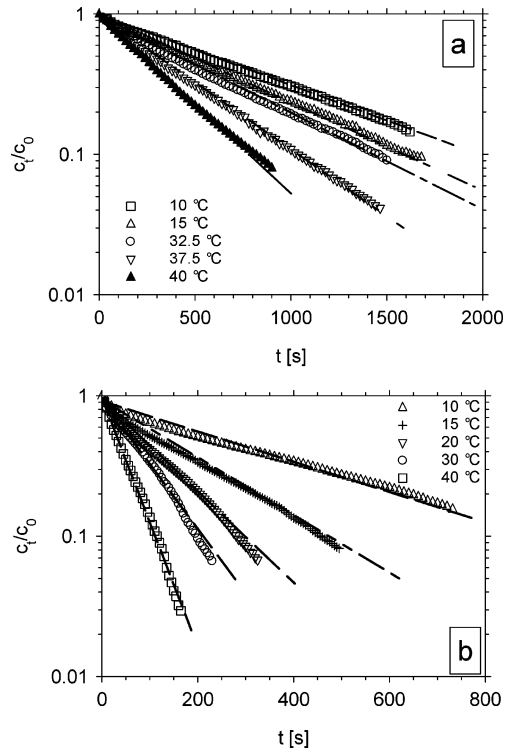

Figure 9. Influence of temperature on the reduction of *p*-nitrophenol on the catalysis of palladium-composites particles. The concentrations of the reactants were as follows: [*p*-nitrophenol] = 0.1 mmol/L, [$NaBH_4$] = 10 mmol/L. (a) Microgel-1-Pd9 system, [Pd composites] = 0.00128 g/L. (b) SPB-30-Pd9 system, [Pd composites] = 0.00063 g/L.

by the insertion of the nanoparticles. Hence, the Pd particles in system 2 are immobilized only by enclosure in the network, not by any chemical binding or strong adsorptive interaction.

Figure 9 shows the dependence of the rate of reaction on temperature. Again the pseudo-first-order kinetics is seen at all temperatures *T*. The dependence of k_{app} on temperature is shown in Figure 10. In the case of system 1, that is, the SPB-30-Pd9 (see Table 2), the rate constant k_{app} that follows from Figure 10 is fully described by a conventional Arrhenius expression with an activation energy E_A = 44 kJ/mol. However, no activation energy could be obtained for system 2, that is, Microgel-1-Pd9 (see Table 2), since k_{app} does not

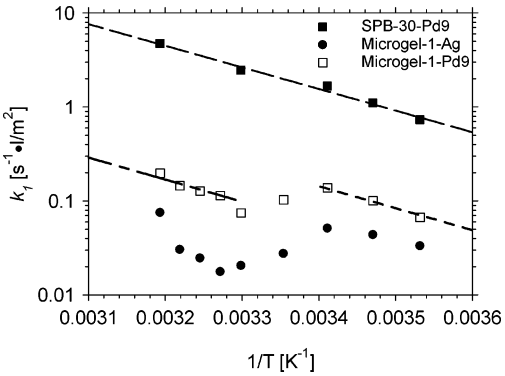

Figure 10. Dependence of the rate constant k_1 (see eq 1) on the temperature *T* for different systems*:* Arrhenius plot of k_1 measured in the presence of the composite particles SPB-30-Pd9 (filled squares; system 1; [Pd composites] = 0.00063 g/L). The activation energy was 44 kJ/mol. In the case of the Microgel-1-Pd9 system (open squares; system 2; [Pd composites] = 0.00128 g/L), we obtained an S-curve, which is similar to that of silver nanoparticles (filled circles; data taken from ref [18]; [Ag composites] = 0.0063 g/L). The concentrations of the reactants were as follows: [*p*-nitrophenol] = 0.1 mmol/L, [$NaBH_4$] = 10 mmol/L.

change with 1/*T* in a linear fashion as is shown in Figure 10. Obviously, the change of temperature not only changes the catalytic activity of the palladium nanoparticles but also leads to a shrinking of the PNIPA network. As a consequence of this, the rate constant decreases because of a diminished diffusion of the reactants similar to the result obtained for silver composite particles.[18,19] However, the catalytic data of Microgel-1-Pd9 could be fitted by the Arrhenius relation if obtained at high or low temperature ($T \leq 20$ °C, $T \geq 32$ °C), that is, in a region not affected by the volume transition region of PNIPA. For this region activation energies of approximately 44 kJ/mol were obtained. Hence, the bare activation energy of composite particles based on SPB or PNIPA systems is the same within the limits of error. This in turn means that the interaction of the reactants with the Pd particles in the PNIPA−Pd composite systems is the same as that of SPB−Pd composite particles. The S-curve seen in the Arrhenius plot in Figure 10 must hence solely be due to the diffusional barrier for the reactants if the network is shrinking with increasing temperature. The much lower activity of the nanoparticles within the PNIPA shell is hence only due to the limitation of diffusion, not to any specific interaction with the PNIPA network.

4. Conclusion

We have presented a study on the catalytic activity of palladium nanoparticles encapsulated in spherical polyelectrolyte brushes and microgels. The reduction of $PdCl_4^{2-}$ ions immobilized in both systems yields nearly monodisperse nanoparticles of metallic palladium (average diameter *d*: 2.4 nm in spherical polyelectrolyte brushes, 3.8 nm in the microgels). The catalytic activity of the Pd nanoparticles was monitored in both systems photometrically by following the reduction of *p*-nitrophenol by $NaBH_4$. The analysis of the kinetic data obtained herein together with data furnished in the literature shows that (i) the catalytic activity of the Pd nanoparticles depends markedly on the type of carrier system used and (ii) the difference in catalytic activity between Pd

nanoparticles in spherical polyelectrolyte brushes and in the PNIPA core−shell particles is only due to a strong limitation of diffusion in the latter system. There is no indication for any specific interaction of the polymer chains with the Pd nanoparticles. Hence, the present study gives clear indications on how carrier systems for metallic nanoparticles should be designed to adjust their catalytic activity.

Acknowledgment. We thank the Deutsche Forschungsgemeinschaft, Sonderforschungsbereich 481, Bayreuth, the European Community, Project "POLYAMPHI", the Fonds der Chemischen Industrie, and the BASF-AG for financial support.

CM062554S